

**N95-19489**

**MICROSTRUCTURALLY BASED VARIATIONS ON THE DWELL FATIGUE LIFE OF TITANIUM ALLOY IMI 834**

113073

Mark L Thomsen

David W. Hoepfner

Quality and Integrity Design Engineering Center

The University of Utah

Salt Lake City, UT

**ABSTRACT**

An experimental study was undertaken to determine the role of microstructure on the fatigue life reduction observed in titanium alloy IMI 834 under dwell loading conditions. The wave forms compared were a trapezoid with 15 and 30 second hold times at the maximum test load and a baseline, 10 Hertz, haversine. The stress ratio for both loading wave forms was 0.10. The fatigue loading of each specimen was conducted in a vacuum within a scanning electron microscope chamber which minimized the possibility that the laboratory environment would adversely affect the material behavior.

Two microstructural conditions were investigated in the experimental program. The first involved standard "disk" material with equiaxed alpha in a transformed beta matrix. The second material was cut from the same disk forging as the first but was heat treated to obtain a martensitic alpha prime microstructure.

Tensile tests were performed prior to the onset of the fatigue loading portion of the study, and it was determined that the yield strengths of the specimens from both material conditions were within ten percent. The maximum fatigue loads were chosen to be 72 percent of the average yield strength for both materials as determined from the tensile tests. It was found that the cycles to failure from the 10 Hertz loading wave form were reduced by a factor of approximately five when the loading was changed to the trapezoidal wave form for the standard "disk" material. The fatigue life reduction for the martensitic structure under identical test conditions was approximately 1.75. The improvement observed with the martensitic structure also was accompanied by an increase in overall fatigue life for the wave forms tested. This paper will review the results and conclusions of this effort.

## INTRODUCTION

Since the development of the gas turbine engine, improvements in engineering alloys, ceramics, and aerodynamics have brought performance levels close to the limits of the materials that are currently available. Because of the wide variety of environmental and loading conditions, various alloy systems are being developed that can withstand very high stresses and high temperatures for an extended period of time. Although the service lives of aeroengines have improved greatly over the past 30 years, life prediction capabilities fall short of maximizing the functionality of critical components [1-5].

In an effort to obtain more service life from the safety critical components in gas turbines, many investigators in the field of fatigue support the use of damage tolerant design [2-6]. Primarily, this involves the use of component life predictions that have been verified by testing. To accomplish this, and get meaningful data, it is necessary to conduct the tests under representative loading and environmental conditions of those experienced in service. Unfortunately, this is costly and time consuming, and in the end, the question of load applicability still exists.

It has been suggested that standardized loading wave forms be used in the testing of components and materials to better characterize their behavior [2,6]. Such programs involve the development of a loading spectrum that is indicative of the actual engine operation. An example of loading spectrum for a military aircraft can be seen in Figure 1 [7]. Although this is much more involved than those for commercial transport aircraft, the concept is the same. Others, however, claim that these spectra may be compressed as shown in Figure 2 which is justified by eliminating the "less severe mission points, e.g. cruise [dwell],..." [1].

The cruise portion of a loading spectrum is important because it requires that the component be under a relatively high load for an extended period of time. Recently, a titanium alloy fan rotor disk failed approximately one hour and seven minutes after takeoff of United Airlines flight 232 [8]. The material the disk was manufactured of contained both the alpha and beta microstructures which have been shown to be sensitive to dwell loading [9-11]. This failure occurred far short of the disk's "rated life" and, ultimately, led to the deaths of 112 people. In sharp contrast to the opinions of some [1,12,13], the importance of the hold time (or dwell period) at some elevated load during operation was shown by this accident.

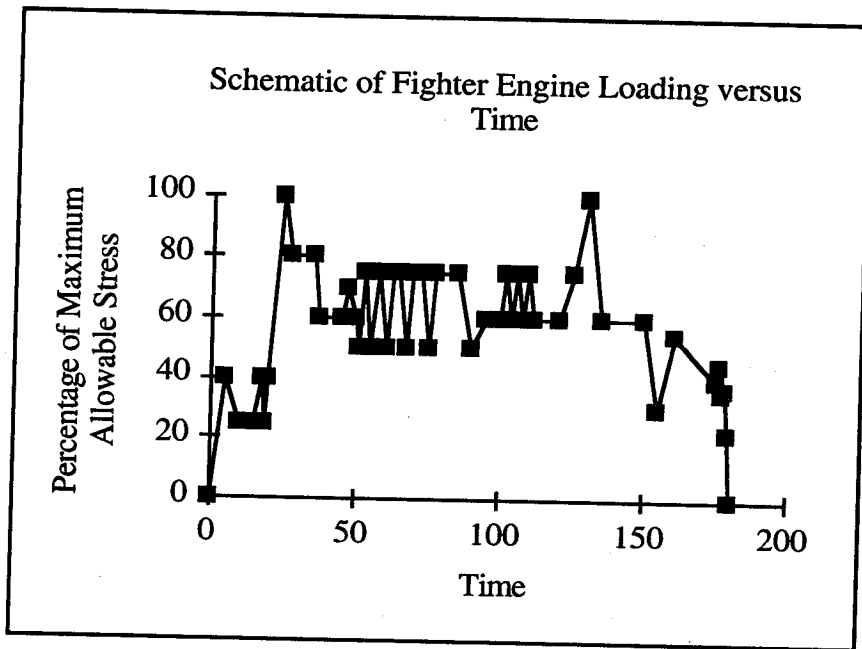


Figure 1. Fighter engine operation spectrum.

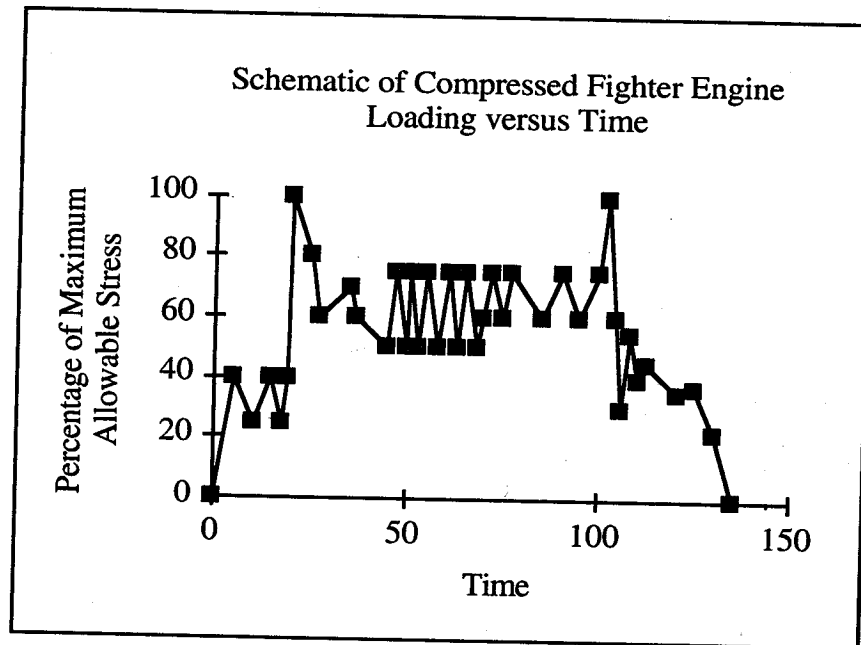


Figure 2. Compressed engine operation spectrum.

## EXPERIMENTAL METHODS

The details of this investigation and the approach taken will be described by section.

### Microstructural Characterization

Two microstructural conditions of IMI 834 were tested. The first was an equiaxed alpha in a transformed beta matrix (disk) with the equiaxed alpha grain dimensions approximately 50  $\mu\text{m}$  and the transformed beta grain dimensions approximately 70  $\mu\text{m}$ . The second was a martensitic alpha prime with grain dimensions on the order of 600  $\mu\text{m}$ . The target composition of the alloy is given in Table 1 [14].

Table 1  
Nominal Composition of IMI 834

| Ti      | Al  | Zr  | Sn  | Nb  | Mo  | Si   |
|---------|-----|-----|-----|-----|-----|------|
| Balance | 5.8 | 3.5 | 4.0 | 0.7 | 0.5 | 0.35 |

In each case the specimen blanks were cut from the bore of the same disk forging. The "disk" specimens then were machined to the specimen geometry with the orientation to the bore of the disk marked for future reference. The specimen blanks from the second microstructural group were cut from the disk forging and then heat treated as to the following schedule: heat 2 hours at 1073 °C, oil quench, age 2 hours at 700 °C, and then air cool. The solution temperature of 1073 °C was chosen since it is 33 °C above the beta transus temperature presented by Bate [15], and complete microstructural transformation was desired. The standard aging temperature and time for the "high alpha-beta" [16] condition was used to allow decomposition of the retained beta phase. Following this heat treatment, the blanks were machined to the specimen geometry to remove the oxygen rich alpha case that often results during heat treating operations [16]. Figures 3 and 4 show the two microstructures used in the study.

### Specimen Geometry

The specimen geometry shown in Figure 5 was chosen because the tests were to be conducted in the vacuum chamber of a scanning electron microscope, the details of which are presented by Stephens and Hoepfner [17], to minimize environmental effects. The groove on the top face of the specimen is oriented towards the bore of the disk as signified by the mark made in the specimen blanks mentioned above. The reason for the groove is to provide a stress state that promotes crack nucleation on the top face

such that it can be viewed in the scanning electron microscope for crack detection and propagation studies. A finite element analysis of the specimen stress state revealed that the presence of the small groove introduced a stress concentration factor of 1.64 near the base of the groove. Since this groove was only on one side of the specimen, the stress concentration diminished to 1.0 at a depth of approximately 0.040 inch.

The surface of the groove was polished to remove any large scratches left over from the final machining operation. This procedure involved a three step wet sanding treatment with 240, 320 and finally 600 grit emery paper. The final polish was with 3  $\mu\text{m}$  diamond paste. This treatment was used for all grooved fatigue test specimens. The tensile test specimens which did not have the groove were tested as received.

### Test Matrix

Since the fatigue response of two microstructural conditions were to be compared, tensile tests were conducted to determine some basic material properties. Although the specimen geometry was not of standard configuration [18], comparative tensile data were obtained on specimens similar to those shown in Figure 5, but without the groove. Again, a finite element analysis of this geometry was conducted to verify that no stress concentration existed and, indeed, none did. Once the approximate tensile data were available, the 0.2 percent offset yield strength was determined.

The fatigue test portion of the study involved a 10 Hertz haversine wave form, trapezoidal wave form with a 15 second hold at the maximum load, and a trapezoidal wave form with a 30 second hold at maximum load, all with a stress ratio of 0.1 and  $\sigma_{\text{max}} = 755 \text{ MPa}$ . All fatigue tests were conducted in a vacuum ( $\approx 10^{-5}$  torr), the details of which are presented in Table 2.

The tensile tests were conducted using a standard electro-hydraulic servo controlled 100 kilo-Newton MTS load frame and extensometer. The fatigue tests were conducted in a specially designed electro-hydraulic servo controlled 25 kilo-Newton "In-Situ" fatigue loading apparatus controlled with standard MTS components.

### Fractography

Fractographic analysis was conducted on the fracture surfaces of the fatigue tested specimens using a Hitachi S-2300 scanning electron microscope operating at 25 kilo-volts. In each case, documentation of the dwell and baseline fracture surface features was made. Comparisons of these features were made and possible reasons for fatigue response variations were drawn.

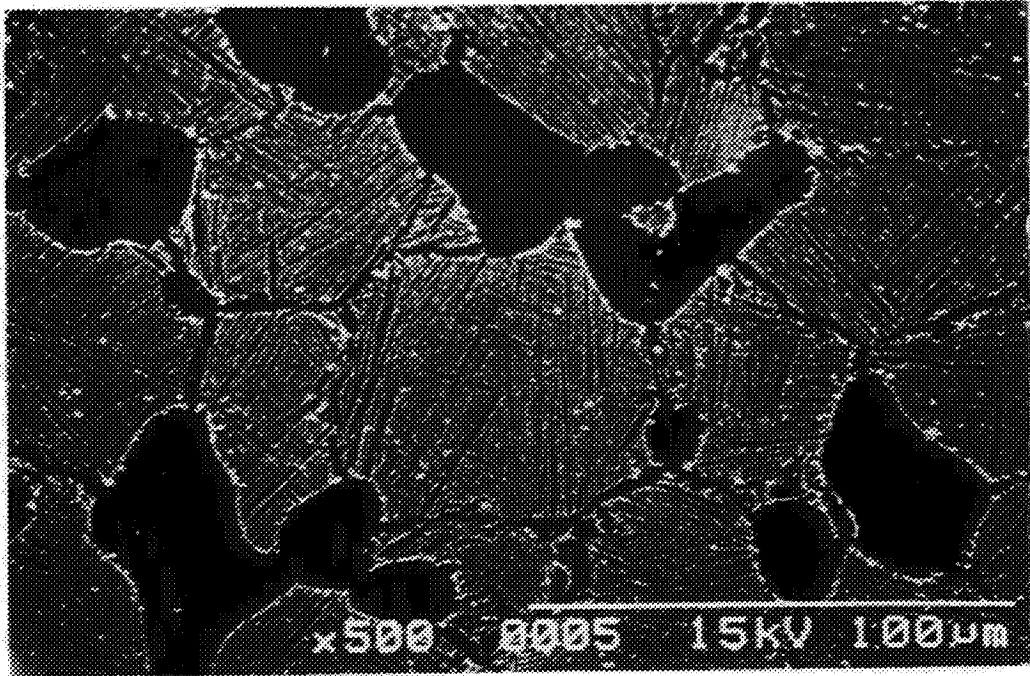


Figure 3. Equiaxed alpha in a transformed beta matrix, "disk" (500X).

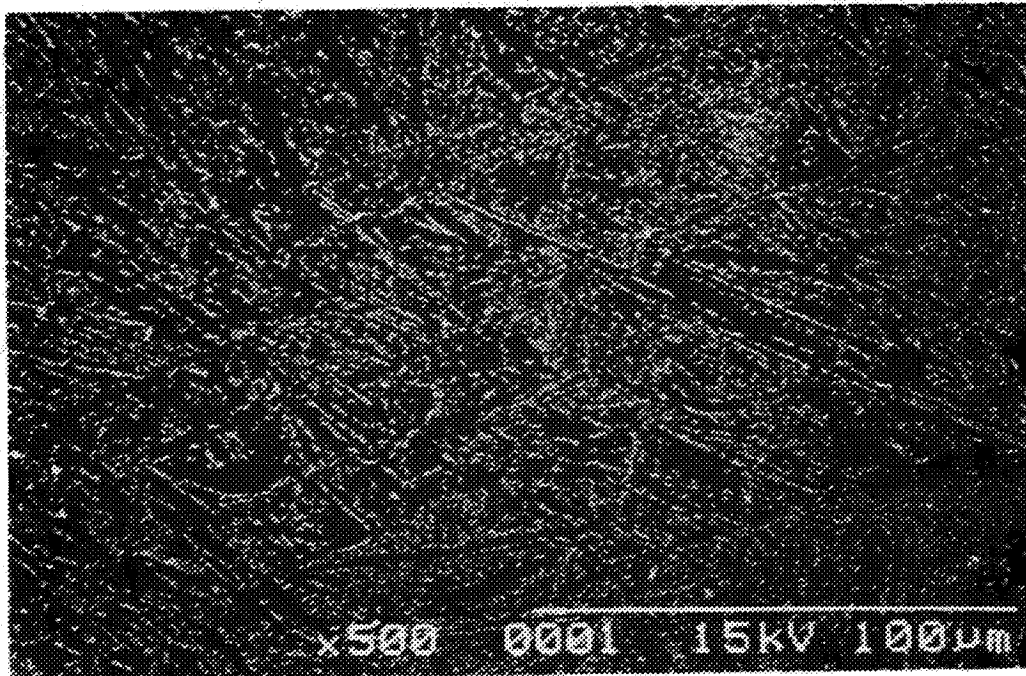


Figure 4. Martensitic alpha prime (500X).

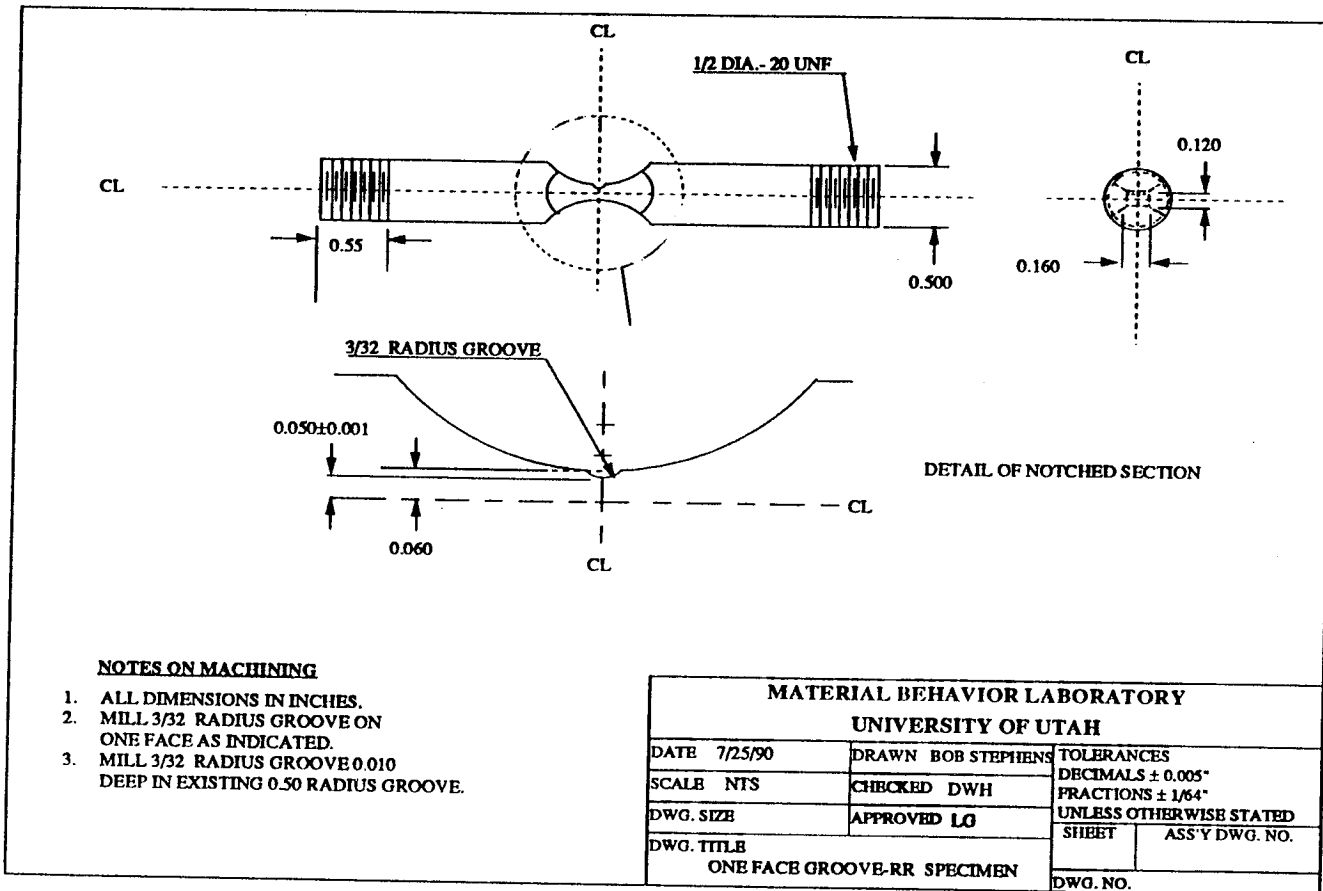


Figure 5. Specimen drawing.

## Results

A summary of the tensile data is shown in Table 3 below, and the fatigue data is shown in Table 4. The values for the total cycles to failure,  $N_f$ , presented are averages obtained from the number of specimens tested for each condition as listed in Table 2.

Table 2  
Overall Experimental Matrix

| Test type | Tests | Wave Form and Environment                        | Microstructural Condition       |
|-----------|-------|--|---------------------------------|
| Tensile   | 1     | N/A Lab Air                                      | Equiaxed Alpha-Transformed Beta |
| Fatigue   | 3     | 10 Hertz Haversine Vacuum                        | Equiaxed Alpha-Transformed Beta |
| Fatigue   | 2     | 0.065 Hertz trapezoid (15 second hold)<br>Vacuum | Equiaxed Alpha-Transformed Beta |
| Fatigue   | 1     | 0.033 Hertz trapezoid (30 second hold)<br>Vacuum | Equiaxed Alpha-Transformed Beta |
| Tensile   | 2     | N/A Lab Air                                      | Martensitic alpha prime         |
| Fatigue   | 2     | 10 Hertz Haversine Vacuum                        | Martensitic alpha prime         |
| Fatigue   | 3     | 0.065 Hertz trapezoid (15 second hold)<br>Vacuum | Martensitic alpha prime         |

Table 3  
Tensile Test Data

| Microstructural Condition       | Specimen | 0.2 Percent Yield Strength<br>(MPa) | Final Strain at Failure<br>( $\mu\epsilon$ ) |
|---------------------------------|----------|-------------------------------------|--|
| Equiaxed Alpha-Transformed Beta | 1        | 1,044                               | 51,458                                       |
| Martensitic Alpha prime         | 1        | 999                                 | 37,041                                       |
| Martensitic Alpha prime         | 2        | 1,110                               | 34,375                                       |



Table 4  
Fatigue Test Data

| Microstructural Condition          | Wave form                                 | Average Cycles to Failure ( $N_f$ ) |
|------------------------------------|---|-------------------------------------|
| Equiaxed Alpha-Transformed<br>Beta | 10 Hertz Haversine                        | 57,372                              |
| Equiaxed Alpha-Transformed<br>Beta | 0.065 Hertz trapezoid<br>(15 second hold) | 13,320                              |
| Equiaxed Alpha-Transformed<br>Beta | 0.033 Hertz trapezoid<br>(30 second hold) | 10,222                              |
| Martensitic Alpha prime            | 10 Hertz Haversine                        | 151,466                             |
| Martensitic Alpha prime            | 0.065 Hertz trapezoid<br>(15 second hold) | 88,277                              |

#### Discussion

The tensile data showed very little difference in the yield strengths between the two microstructures. The strain data of the martensitic specimens, however, was significantly different. This is most likely related to the non-standard heat treatment for this alloy. Typically, solution treating above the beta transus for near alpha alloys results in superior creep resistance at the expense of fatigue properties and deformation characteristics, as shown by the tensile data. However, aging at 700 °C for this particular alloy results in improved fatigue properties while maintaining much of the creep resistance [16] with some loss in total deformation to failure.

From the above, it is expected that the fatigue properties would be comparable between the two microstructures. The advantages of the disk microstructure, equiaxed alpha in a transformed beta matrix, are improved creep resistance, tensile properties, fatigue properties, and fracture toughness [15,19]. Although this was the case, the study shows that for the test conditions employed, the martensitic microstructural condition out performs the disk microstructure.

The observed fatigue life reduction associated with the dwell (hold time) at maximum load has been observed by several others at room temperature. An additional observation associated with this phenomenon is the temperature dependence and the fact that this fatigue life reduction under dwell is diminished as temperature is increased. Reports of this saturation temperature have been from 75-200 °C. Some of the mechanisms that have been proposed are:

- hydrogen embrittlement at, and immediately ahead of, the crack tip by a dislocation locking mechanism which is unlocked at elevated temperature [10],

- hydride formation along the basal planes of the alpha phase and subsequent cracking of these hydrides (related to volumetric misfit between hydride and alpha phase) [20,21],
- hydrogen embrittlement at, and ahead of, the crack tip enhanced by the strain induced increase in the diffusion rate of hydrogen to these zones and subsequent cracking of hydrides that may form [22],
- creep, or strain accumulation, during the dwell period with inclusion of the microstructural "weak link" concept that assists in explaining the effect of specimen size [23], and
- hydrogen assisted grain boundary sliding [24].

Other observations have included that the content of primary alpha influences the degree of the dwell effect [10] on fatigue lives of titanium alloys.

Fractographic observations comparing the fracture surfaces of dwell and non-dwell specimens have noted several features of the dwell specimens. Some of the more prominent observations are [10,23,25]:

- increased faceting oriented approximately normal to the loading axis,
- facet planes are associated with the basal planes of the alpha phase,
- secondary cracking, similar to that observed in embrittled materials, and
- coarsening of the fracture surface features.

With these in mind, it has been reported [25] that a distinct change in crack growth mechanism occurs between dwell and non-dwell specimens.

The degree of fatigue life reduction observed in this study was by a factor of approximately five for the disk specimens and only a factor of 1.7 for the martensitic specimens. Part of this variation can be explained by considering some of the proposed mechanisms.

Each of the specimens are from the same disc, so it is reasonable to assume the internal hydrogen content is similar. Even though subsequent heat treatment was performed to obtain the martensitic specimens, this was done prior to machining. During the machining process, approximately 0.25 inch of material was removed. This would reduce the chance for significant hydrogen pickup during the heat treatment to penetrate to the depth required to influence the behavior of the specimen across the gage section. Therefore, the probability of significant variations in hydrogen content within the two separate microstructural groups is remote.

In examining the fractographic evidence, it is apparent that coarsening of the fracture surface does, indeed, occur as mentioned above. In comparing Figures 6 and 7 to Figures 8 and 9, this coarsening is apparent. Striations were found along the non-dwell fracture surface, Figure 7, that were not observed on dwell fracture surfaces. The secondary cracking associated with the dwell surface was not observed on the non-dwell surface. Increased faceting on the dwell surface is a product of the coarsening mentioned above. The size of the facet planes often corresponded to the size of the near alpha grains. In general, the fracture surface of the non-dwell specimen can be characterized as showing more deformation with some

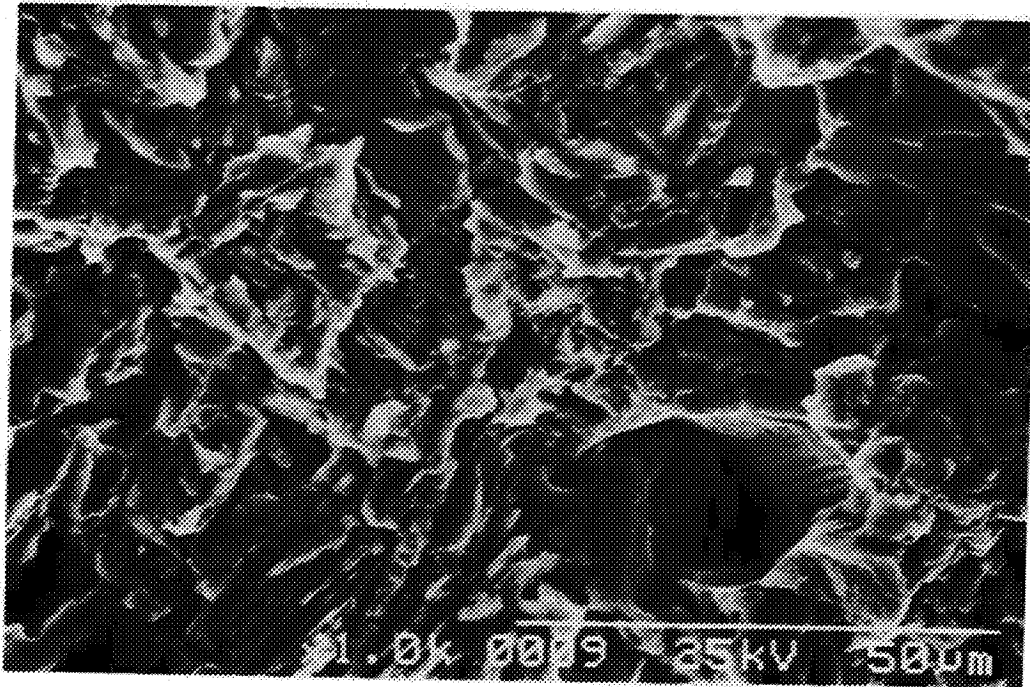


Figure 6. Fracture surface of the Disk specimen with a 10 Hertz haversine fatigue loading wave form (1000X).

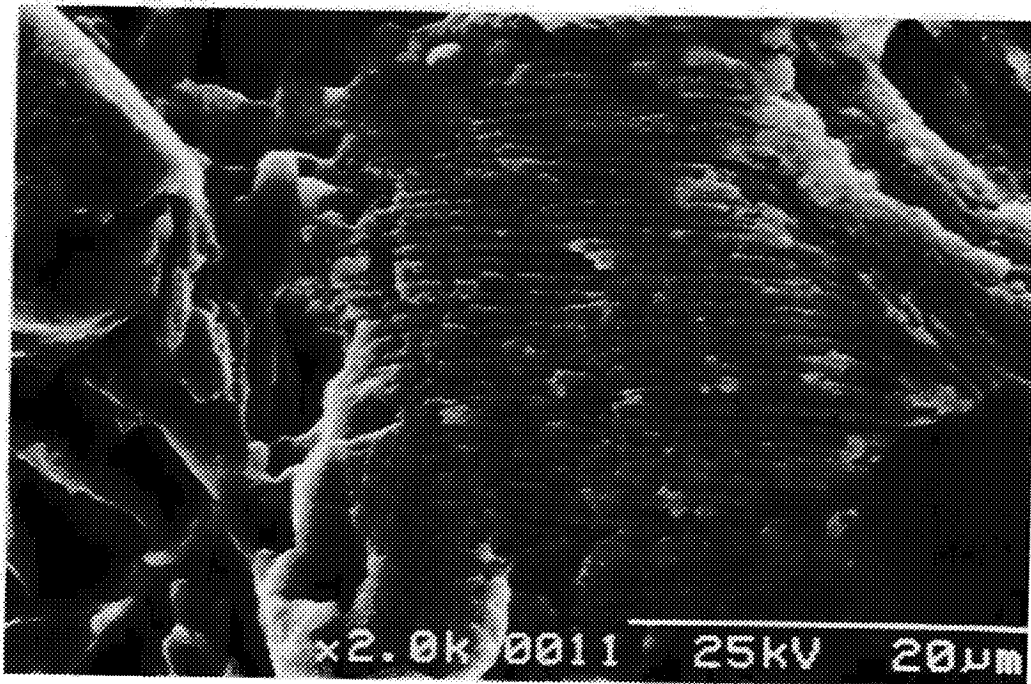


Figure 7. Striation field near the fast fracture zone of the Disk specimen with a 10 Hertz haversine fatigue loading wave form (2000X).

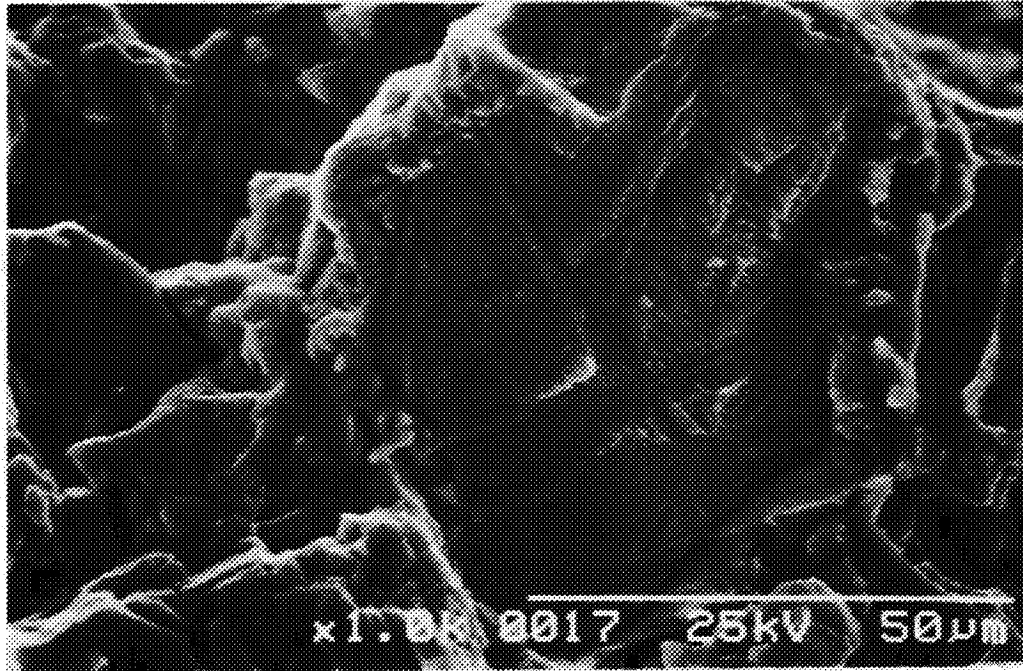


Figure 8. Secondary cracking and cleavage planes on the fracture surface of the Disk specimen tested at 0.065 hertz (Dwell) (1000X).

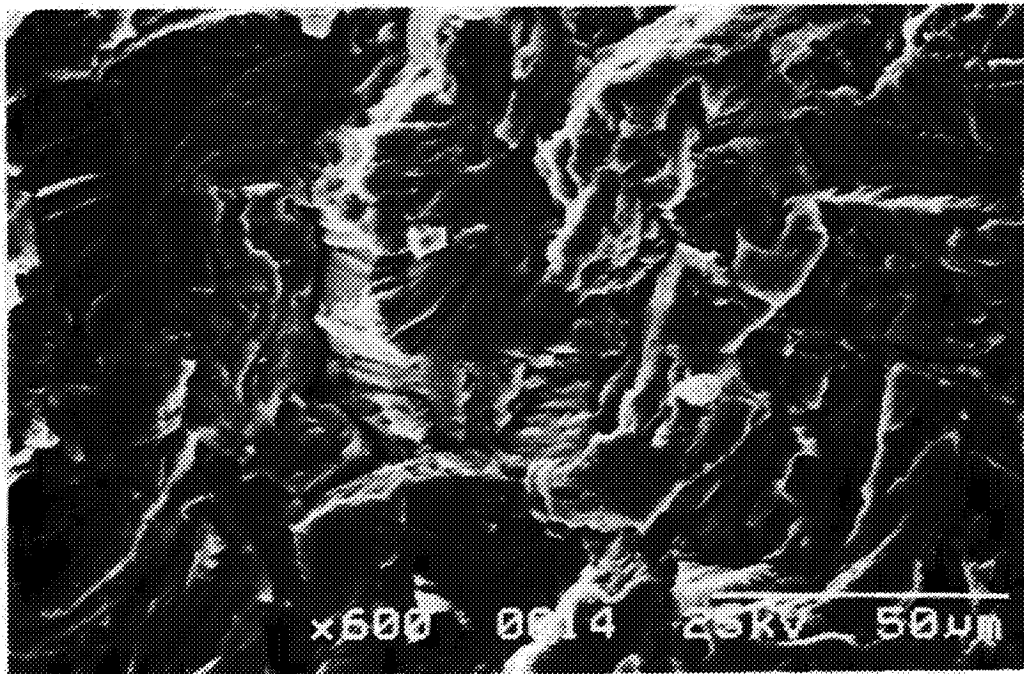


Figure 9. More secondary cracking on the fracture surface of the Disk specimen tested at 0.065 hertz (Dwell) (600X).

striation fields. The dwell specimen surface is predominately quasi-cleavage with very little sign of deformation.

The martensitic fracture surfaces showed distinct microstructural dependence as shown in Figures 10 and 11. The dwell fracture surfaces, Figures 12 and 13, were very similar to the non-dwell surfaces with the exception of numerous craters in the surface associated with very limited secondary cracking as compared to the disk microstructure. In comparison of the fracture surfaces at higher magnification, Figures 11 and 13, very little difference in cracking mechanisms is apparent on the micro-mechanics level. Overall, the fracture surface characterization is predominately transgranular.

An observation made by Song and Hoepfner [26] was that the size of the specimen has an effect on the dwell life reduction observed in other titanium alloys. In this study, three different specimens were tested at three separate stress levels. The findings were that as the specimen size was reduced, a more pronounced dwell life reduction was observed for all stresses tested. The conclusion drawn from this was that dwell effect was related to the degree of coarseness of the microstructure and that the increased prior beta grains tend to impede the deformation under uniaxial loading conditions.

Past In-Situ fatigue crack propagation studies by Stephens and Hoepfner [27] of the disk microstructure has shown an increased tendency for crack nucleation to be associated with the primary alpha grains for non-dwell tests. For the dwell tests, crack nucleation sites were found in both the transformed beta and the alpha phases. Crack growth was found to be planar in the alpha phase and more tortuous in the transformed beta phase. Although an etchant was used, no difference in fatigue life was observed.

In-Situ fatigue crack propagation studies in the martensitic structure were difficult. In comparison to the unetched specimens used for the fatigue study, a pronounced life reduction was encountered when an etchant was used to highlight the microstructural features. This has been observed before by Ryder et. al. [28] and one possible explanation may be related to preferential attack of the alpha prime phase by the etchant. If this occurred, it would be expected that crack nucleation and propagation would be influenced by the orientation of the alpha prime plates with respect to the loading axis. Although the etchant was present, it was observed that crack propagation along the alpha prime plates oriented nearly perpendicular to the loading axis was noticeably faster than those plates oriented nearly parallel to the loading axis. This micro-structurally dependent crack path morphology is shown in Figure 14.

The additional life reduction associated with disk specimens by changing the dwell time at maximum load from 15 to 30 seconds was minimal. This was first noted by Ryder et. al. [28] in 1973. This study mentioned that the maximum effect occurred between 15 seconds and one minute. This would indicate that the mechanisms responsible for this substantial life reduction may be related to dislocation locking, as mentioned above, rather than cold creep. If it was entirely creep related, the tendency for fatigue life reduction would continue with longer periods of hold at maximum load. Therefore, a saturation time would not be achieved, as was shown here and in the work of Ryder et. al.

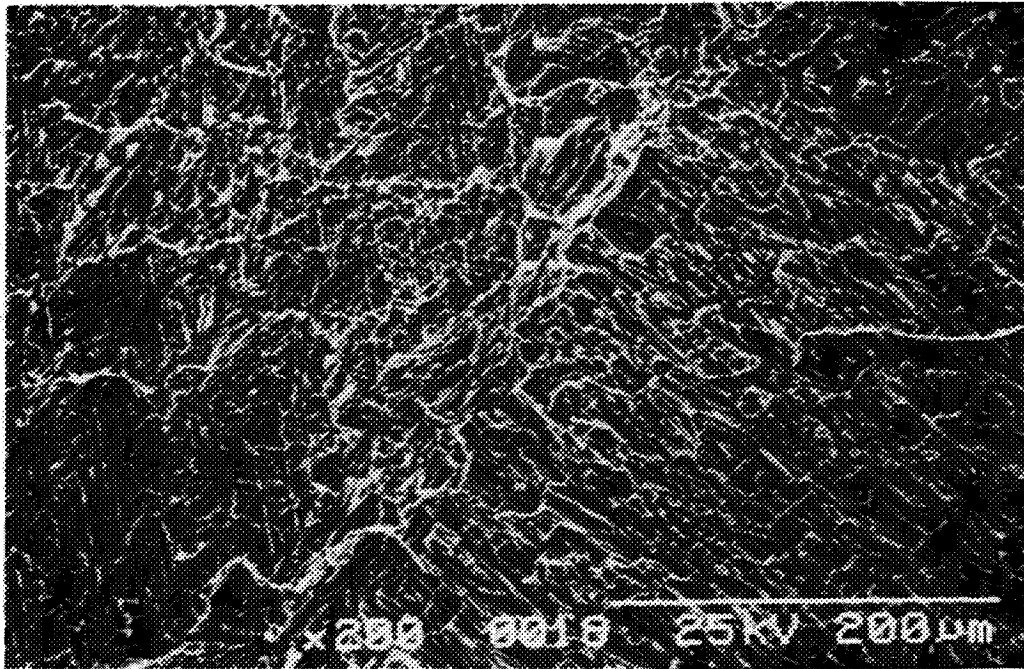


Figure 10. Fracture surface of the martensitic alpha prime condition specimen with a 10 Hertz haversine fatigue loading wave form (200X).

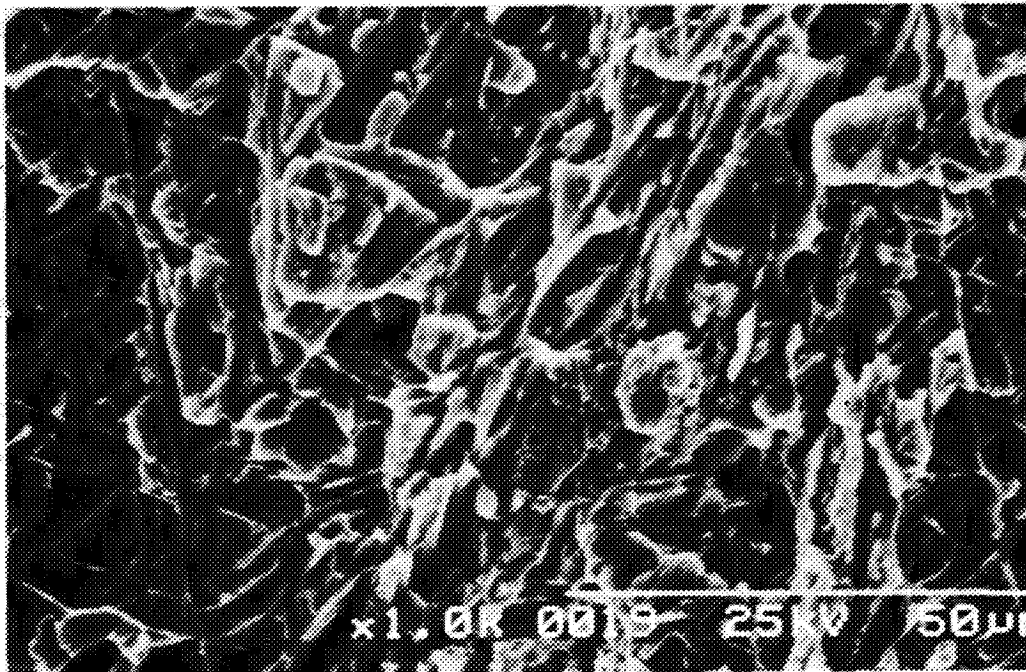


Figure 11. Close up of the martensitic alpha prime fracture surface tested with a 10 Hertz haversine fatigue loading wave form (1000X).

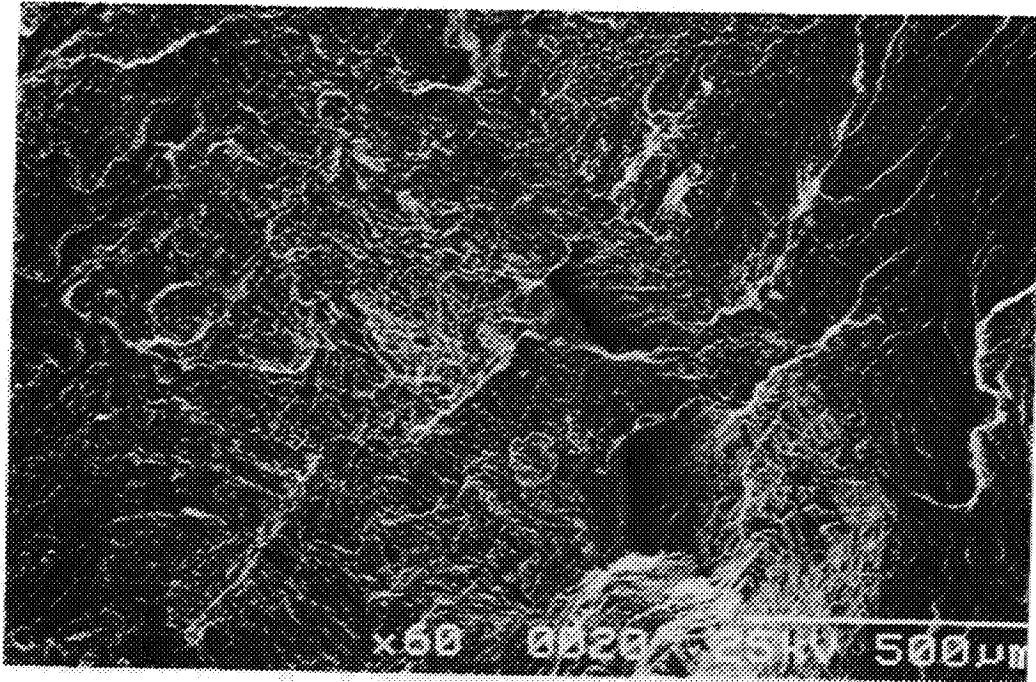


Figure 12. Fracture surface of the martensitic alpha prime condition specimen with a 0.065 Hertz trapezoidal fatigue loading wave form (60X).

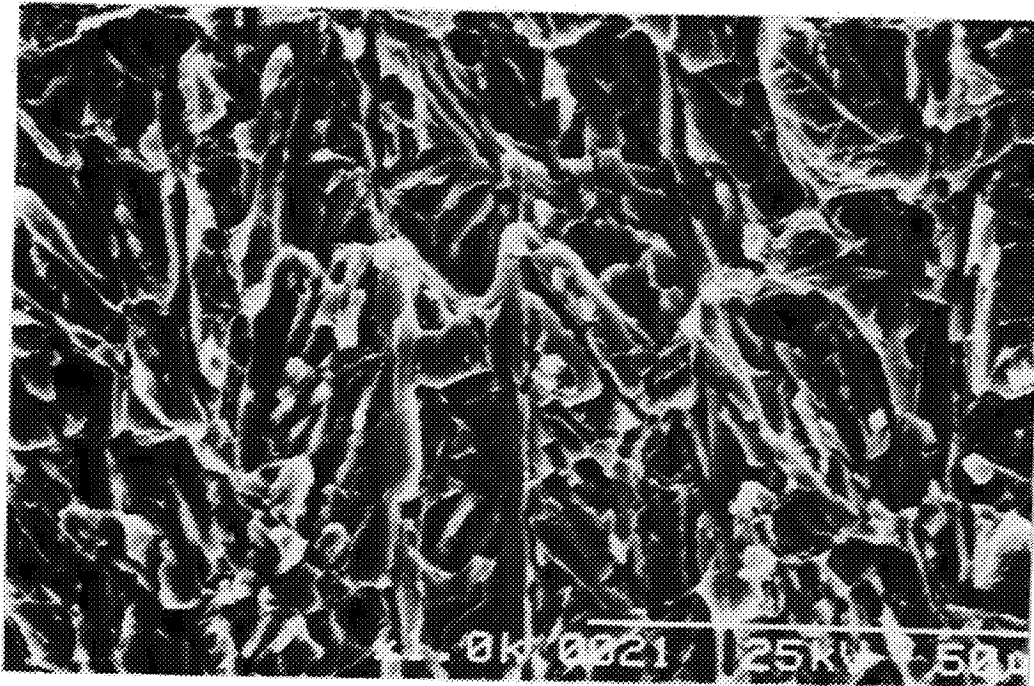


Figure 13. Close up of the martensitic alpha prime fracture surface tested with a 0.065 Hertz trapezoidal fatigue loading wave form (1000X).

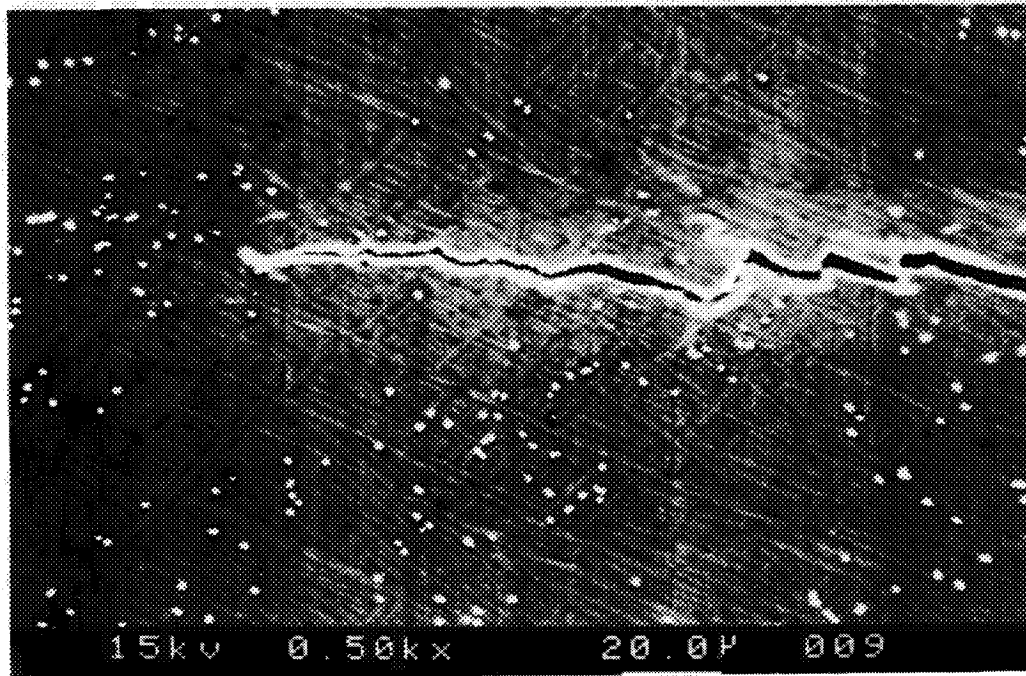


Figure 14. Alpha prime plate orientation influence on the growth of a fatigue crack in an etched specimen (etchant 3 HF-6 HNO<sub>3</sub>-100 H<sub>2</sub>O at 500X).



## Conclusions

The observations made in this investigation are summarized below.

1. Comparable tensile properties to the disk microstructure, equiaxed alpha in a transformed beta matrix, can be obtained from a martensitic microstructure when aged at the "high alpha-beta" aging temperature. Improved fatigue response is achieved, as well, with approximately 30 percent loss in total strain to failure.
2. Martensitic alpha prime showed much less reduction in life compared to the disk microstructure when a dwell time at maximum load was imposed.
3. Very little difference in fracture surfaces was noticed for the two separate loading conditions tested for the martensitic microstructure indicating only subtle changes in crack growth mechanisms.
4. Substantial secondary cracking was found on the fracture surface of the disk microstructure specimens tested with a dwell time at maximum load which was not present in the non-dwell tests.
5. Fatigue life variation between 15 and 30 second dwell tests for the disk microstructure was minimal indicating a saturation time for observation of the dwell induced fatigue life reduction may exist.
6. The mechanisms responsible for the dwell effect in titanium alloys at temperatures less than approximately 200 °C are not entirely related to the room temperature creep, that is also observed in these materials.

## Acknowledgments

Thanks are extended to the Quality and Integrity Design Engineering Center and FASIDE International, Inc. for providing equipment and support throughout this research program, Steven Kinyon for assistance during fractographic documentation, and Tom Mills for assistance in preparation. Thanks are also extended to Dr. Leon Grabowski of Rolls Royce plc for his suggestions, comments, and for providing specimens used in this investigation.

## References

1. Farmer, T.E.: View of Future Requirements for Engine Cyclic Durability by Analysis and Testing, *AGARD Conference Proceedings n 368 Publ by AGARD*, Neuilly-sur-Seine, Fr Available from NTIS, Springfield, VA, USA, 1984, p 20 1-20 6.
2. Taylor, W.R.: Accelerated Mission Endurance Testing (AMET), *AGARD Conference Proceedings n 368 Publ by AGARD*, Neuilly-sur-Seine, Fr Available from NTIS, Springfield, VA, USA, 1984, p 3 1-3 5.

3. Hoepfner, D.W.: History and Prognosis of Material Discontinuity Effects on Engine Components Structural Integrity, *74th AGARD/SMP Meeting on Impact of Materials Defects on Engine Structures*, Keynote Address, Patras, Greece, May 27-28, 1992, p 1 1-1 8.
4. Jeal, R.H.: Relationship Between Fatigue Modeling and Component Integrity, *Fatigue 84*, Publ by Engineering Materials Advisory Services Ltd, Engl, 1984, p 1865-1879.
5. Evans, W.J.; Smith, M.E.F.; Williams, C.H.H.: Disc Fatigue Life Predictions for Gas Turbine Engines, *AGARD Conference Proceedings n 368 Publ by AGARD*, Neuilly-sur-Seine, Fr Available from NTIS, Springfield, VA, USA, 1984, p 11 1-11 13.
6. Hill, R.J.: Verification of Life Prediction Through Component Testing, *AGARD Conference Proceedings n 368 Publ by AGARD*, Neuilly-sur-Seine, Fr Available from NTIS, Springfield, VA, USA, 1984, p 17 1-17 9.
7. Larsen, J.M.; Nicholas, T.: Cumulative Damage Modeling of Fatigue Crack Growth, *AGARD Conference Proceedings n 368 Publ by AGARD*, Neuilly-sur-Seine, Fr Available from NTIS, Springfield, VA, USA, 1984, p 11 1-11 13.
8. Aircraft Accident Report, PB 90-910406, NTSB/AAR-90/06, [Re:UA Flight 232] Accident July 19, 1989, Report Date November 1990.
9. Evans, W.J.; Smith, M.E.F.; Williams, C.H.H.: Fatigue Performance of Discs and Engineering Specimens, *Fatigue 84*, Publ by Engineering Materials Advisory Services Ltd, Engl, 1984, p 1325-1335.
10. Stubbington, C.A.; Pearson, S.: Effect of Dwell on the Growth of Fatigue Cracks in Ti-6Al-4V, *Engineering Fracture Mechanics*, v 10, p 723-756.
11. Song, Z.; Hoepfner, D.W.: Dwell Time Effects on the Fatigue Behaviour of Titanium Alloys, *International Journal of Fatigue*, v 10 n 4, Oct 1988, p 211-218.
12. Bania, P.J.; Eylon, D.: Fatigue Crack Propagation of Titanium Alloys Under Dwell-Time Conditions, *Metallurgical Transactions A*, 9A, June 1978, p 847-855.
13. Sommer, A.W.; Eylon, D.: On Fatigue Crack Propagation of Titanium Alloys Under Dwell Time Conditions, *Metallurgical Transactions A*, 14A, October 1983, p 2178-2181.
14. Daeubler, M.A.; Walker, N.A.; Cope, M.T.: Influence of Heat Treatment on Microstructure and Properties of an Advanced High Temperature Titanium Alloy, *Sixth World Conference on Titanium*, France 1988.
15. Bate, P.S.; Blackwell, P.L.; Brooks, J.W.: Thermomechanical Processing of Titanium IMI 834, *Sixth World Conference on Titanium*, France 1988, p 287-292.
16. ASM Handbook: Volume 4-Heat Treating, ASM International, 1991, p. 913-923.
17. Stephens, R.R.; Hoepfner, D.W.: A New Apparatus for Studying Fatigue Deformation at High Magnifications, *Review of Scientific Instruments*, Vol. 59, No. 8, August, 1988, p. 1412-1419.

18. Standard Test Method for Tension Testing of Metallic Materials, 1993 Annual Book of ASTM Standards, American Society of Testing and Materials, Vol. 3.01, 1993, p. 130-149.
19. Neal, D.F.: Development and Evaluation of High Temperature Titanium Alloy IMI 834, *Sixth World Conference on Titanium*, France 1988, p 253-258.
20. Numakura, H.; Koiwa, M.: Hydride Precipitation in Titanium, *Acta Metallurgica*, v 32 n 10, Oct 1984, p 1799-1807.
21. Sommer, A.W.; Froes, F.H.; Eylon, D.: On the Incidence of Near Basal Cleavage During the Growth of Fatigue Cracks in Alpha Plus Beta Ti Alloys, Publ by ASM, Metals Park, OH, USA, p 83-87, 1986.
22. Hack, J.E.; Leverant, G.R.: A Model For Hydrogen-Assisted Crack Initiation of Planar Shear Bands in Near-Alpha Titanium Alloys, *Scripta Metallurgica*, v14, 1980, p 437-441.
23. Harrison, G.F.; Trantner, P.H.; Winstone, M.R.; Evans, W.J.: The influence of Low Temperature Cyclic Creep on the Fatigue Resistance of a Near-Alpha Titanium Alloy, *Proceedings of the Second International Conference on Creep and Fracture of Engineering Materials and Structures*, Pt. 1, Pineridge Press, Ltd, Swansea, Wales, 1987 p. 395-406.
24. Margolin, H.: Hydrogen Sliding at Alpha/Beta Interfaces of Titanium Alloys, *Scripta Metallurgica et Materialia*, v 24, 1990, p. 2397-2400.
25. Hoepfner, D.W.: A Fractographic Analysis of Flaw Growth in a High Strength Titanium Alloy, *Metallography*, Vol. 11, 1978, p. 129-154.
26. Song, Z., Hoepfner, D.W.: Size Effect on the Fatigue Behaviour of IMI 829 Titanium Alloy Under Dwell Conditions, *International Journal of Fatigue*, v 11 n 2, Mar 1989, p 85-90.
27. Stephens, R.R.; Hoepfner, D.W.: unpublished work conducted at the Quality and Integrity Design Engineering Center, The University of Utah, Salt Lake City, Utah, 1992.
28. Ryder, J.T.; Pettit, D.E.; Krupp, W.E.; Hoepfner, D.W.: *Final Report: Evaluation of Mechanical Property Characteristics of IMI 685*, Lockheed-California Company, Rye Canyon Laboratory, October 1973.